

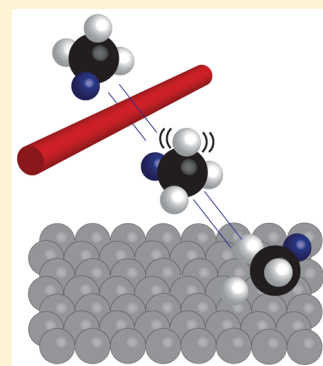
# Bond-Selective and Mode-Specific Dissociation of CH<sub>3</sub>D and CH<sub>2</sub>D<sub>2</sub> on Pt(111)

P. Morten Hundt,<sup>†,§</sup> Hirokazu Ueta,<sup>†,||</sup> Maarten E. van Reijnen,<sup>†</sup> Bin Jiang,<sup>‡</sup> Hua Guo,<sup>‡</sup> and Rainer D. Beck<sup>\*,†</sup>

<sup>†</sup>Laboratoire de Chimie Physique Moléculaire, Ecole Polytechnique Fédérale de Lausanne, Lausanne 1015, Switzerland

<sup>‡</sup>Department of Chemistry and Chemical Biology, University of New Mexico, Albuquerque, New Mexico 87131, United States

**ABSTRACT:** Infrared laser excitation of partially deuterated methanes (CH<sub>3</sub>D and CH<sub>2</sub>D<sub>2</sub>) in a molecular beam is used to control their dissociative chemisorption on a Pt(111) single crystal and to determine the quantum state-resolved dissociation probabilities. The exclusive detection of C–H cleavage products adsorbed on the Pt(111) surface by infrared absorption reflection spectroscopy indicates strong bond selectivity for both methane isotopologues upon C–H stretch excitation. Furthermore, the dissociative chemisorption of both methane isotopologues is observed to be mode-specific. Excitation of symmetric C–H stretch modes produces a stronger reactivity increase than excitation of the antisymmetric C–H stretch modes, whereas bend overtone excitation has a weaker effect on reactivity. The observed mode specificity and bond selectivity are rationalized by the sudden vector projection model in terms of the overlap of the reactant's normal mode vectors with the reaction coordinate at the transition state.



## INTRODUCTION

Ever since the invention of the laser in 1960, chemists have strived toward laser control of chemical reactions. Starting in 1990, the groups of Crim and Zare<sup>1,2</sup> reported a number of bond-selective bimolecular reactions in the gas phase demonstrating that bond selectivity can be achieved via selective vibrational reactant excitation. In addition to realizing the 30 year old dream of laser controlled reactions, the investigation of vibrational control of reaction probabilities (mode specificity) and branching ratios (bond selectivity) provides detailed insight into the microscopic dynamics of a chemical reaction. More recently it was demonstrated that mode specificity and bond selectivity are not limited to gas-phase reactions but can be observed also in gas–surface reactions.<sup>3,4</sup> The dissociative chemisorption of methane on transition metal surfaces has become a prototype system to investigate mode selectivity and bond specificity in gas–surface reactions in both experiment and theory.<sup>5</sup> A detailed understanding of methane chemisorption is of great practical interest because this reaction is known to be the rate-limiting step in the steam reforming process for industrial hydrogen production.<sup>6</sup>

Partially deuterated species are particularly well suited to explore mode- and bond-selective reactivity. A first case of bond selectivity in a bimolecular gas-phase reaction was reported by Crim and co-workers<sup>7</sup> for HOD where a strong preference for the cleavage of the O–H bond was observed in the hydrogen abstraction reaction by H atoms when the O–H bond was vibrationally excited to a localized O–H stretch overtone.

For a reaction to be mode-specific, the reaction probability does not simply depend on the total vibrational energy content but on the specific vibrational quantum state of the reactant. Two iso-energetic reactant states can lead therefore to rather

different reaction probabilities. One example of a mode-specific gas-phase reaction is the H-abstraction reaction of CH<sub>3</sub>D by a chlorine atom, reported by Yoon et al.<sup>8,9</sup> The authors used their state-resolved reactivity data to calculate state-specific reaction cross sections for the  $\nu_1$ ,  $\nu_4$  and  $2\nu_5$  normal modes of CH<sub>3</sub>D. They find the symmetric stretch vibration ( $\nu_1$ ) to be 7 times more reactive than the antisymmetric stretch ( $\nu_4$ ) whereas the bending overtone ( $2\nu_5$ ) had no detectable influence on the reactivity. Furthermore, the reaction of vibrationally excited CH<sub>3</sub>D with chlorine was reported to be bond-selective.<sup>10</sup> The reaction of vibrationally excited CH<sub>2</sub>D<sub>2</sub> with chlorine atoms was also reported to be bond- and mode-selective.<sup>11,12</sup> The group of Richard Zare<sup>11,12</sup> showed that upon excitation of the first C–H stretch overtone in CH<sub>2</sub>D<sub>2</sub> a C–H bond breaks preferentially whereas upon C–D stretch excitation a C–D bond breaks preferentially. In addition, they found that excitation of the  $|20\rangle$  C–H stretching mode of CH<sub>2</sub>D<sub>2</sub> shows different rotational distributions, vibrational distributions, and scattering angles of the reaction products than excitation of the  $|11\rangle$  mode.

Despite their larger complexity, experiments performed on gas–surface reactions show many parallels to the findings obtained in bimolecular gas-phase reactions. In 2003 vibrational mode-specific reactivity of doubly deuterated methane on a nickel single-crystal surface was reported<sup>13</sup> and several studies

**Special Issue:** Dynamics of Molecular Collisions XXV: Fifty Years of Chemical Reaction Dynamics

**Received:** August 14, 2015

**Revised:** September 28, 2015

of mode-specific methane/transition metal surface reactions followed.<sup>14–17</sup>

In 2008 the first example of vibrational bond selectivity on surfaces was reported in the dissociative chemisorption of CHD<sub>3</sub> on Ni(111).<sup>3</sup> Recently, our laboratory at EPFL presented a study<sup>4</sup> where reflection–absorption infrared spectroscopy (RAIRS) was used to directly detect the nascent products of methane dissociation on Pt(111). The dissociation of all three partially deuterated methane isotopologues (CH<sub>3</sub>D ( $\nu_4$ ), CH<sub>2</sub>D<sub>2</sub> ( $\nu_6$ ), and CHD<sub>3</sub> ( $\nu_1$ )) was discovered to be highly bond-selective for C–H stretch excitation. The experimentally observed bond selectivity on Ni(111) was simulated by using quasi-classical trajectories on a global potential energy surface (PES),<sup>18</sup> and the simulation results are consistent with the experiment.<sup>19</sup>

In this article, we present experimental data that show that the dissociative chemisorption of CH<sub>3</sub>D and CH<sub>2</sub>D<sub>2</sub> on Pt(111) is highly bond-selective for excitation of different vibrational eigenstates. Furthermore, we used RAIRS to measure state-resolved sticking coefficients of the three mentioned vibrational states and thereby demonstrate that the reactions are mode-specific. To rationalize the experimental findings, we have used the recently proposed sudden vector projection (SVP) model, which assumes the reaction occurs in the sudden limit and attributes the vibrational enhancement of reactivity to the coupling of the reactant mode with the reaction coordinate at the transition state.<sup>20,21</sup>

## EXPERIMENTAL SECTION

The experiments reported here were performed in a molecular beam/surface science apparatus that is described in more detail elsewhere.<sup>22</sup> Therefore, we only briefly summarize its most important features and the experimental procedure used here. A triply differentially pumped molecular beam source is coupled to a UHV chamber containing a single crystal surface mounted on a home-built four-axis manipulator. The sample mounting allows for heating to 1300 K and cooling to 78 K. During the experiments reported here, the temperature was stabilized to 150 ± 0.1 K. Adsorbed products of the dissociative chemisorption of methane are detected by reflection absorption infrared spectroscopy (RAIRS) using a Fourier transform infrared spectrometer (FTIR) (Bruker Vertex 70v) with an external InSb detector. RAIRS provides a noninvasive method for the online detection of the adsorbed methyl (CH<sub>x</sub>D<sub>y</sub>,  $x + y = 3$ ) species produced by the dissociative chemisorption of incident methane on the cold Pt(111) surface. Auger electron spectroscopy (AES) was used to calibrate the RAIRS signals for the different methyl isotopologues in terms of surface coverage  $\theta$ .<sup>22</sup>

A continuous molecular beam of either singly and doubly deuterated methane (99% isotopic purity) was formed by expanding 3% CH<sub>3</sub>D or CH<sub>2</sub>D<sub>2</sub> seeded in helium (3 bar, 300 K) through a 50  $\mu$ m diameter nozzle and a 2 mm diameter skimmer. Velocity distributions of the molecular beam were measured by an on-axis quadrupole mass spectrometer in combination with a fast chopper wheel. At a nozzle temperature of 300 K the average translational energy of CH<sub>3</sub>D and CH<sub>2</sub>D<sub>2</sub> was determined to be 24 ± 4.5 kJ/mol.

The methane isotopologues were prepared in specific ro-vibrational eigenstates by intersecting the molecular beam between nozzle and skimmer with infrared radiation from a tunable continuous wave single mode optical parametric oscillator (cw-IR OPO). The OPO idler output was frequency

stabilized to ±1 MHz by locking to a Doppler-free saturation hole (Lamb-dip) detected in a static gas cell. Excitation of the molecular beam occurred by rapid adiabatic passage using a cylindrical lens ( $f = +25$  cm) to gently focus the IR beam into the interaction region with the molecular beam. The focusing creates curved wavefronts that lead to a Doppler frequency tuning effect as the reactant molecules pass through the divergent IR beam. Under suitable conditions the frequency chirp will invert the reactant population from the ground state to a ro-vibrationally excited state by rapid adiabatic passage (RAP).<sup>23</sup> Three different ro-vibrational eigenstates of CH<sub>3</sub>D and two eigenstates of CH<sub>2</sub>D<sub>2</sub> were prepared in the molecular beam by excitation of the R<sub>0</sub>(1) transitions originating from  $J = 1$ ,  $K = 0$  of the symmetric top molecule CH<sub>3</sub>D and R<sub>01</sub>(1) transitions of the asymmetric top molecule CH<sub>2</sub>D<sub>2</sub>. The incident flux of CH<sub>3</sub>D or CH<sub>2</sub>D<sub>2</sub> was monitored by measuring the partial pressure of the respective gas in the UHV chamber with a quadrupole mass spectrometer. A room temperature pyroelectric detector that could be translated into the molecular beam to measure its vibrational energy content was used to determine the fractions of state prepared CH<sub>3</sub>D or CH<sub>2</sub>D<sub>2</sub> in the molecular beam. The measured flux of excited molecules incident on the surface was used with the resulting methyl product coverage on the surface obtained from the calibrated RAIRS detection to determine the absolute reaction probabilities and branching ratios for C–H and C–D cleavage.

## RESULTS

**State-Resolved Dissociation of CH<sub>3</sub>D.** Comparison of the five RAIR spectra shown in Figure 1 demonstrates the

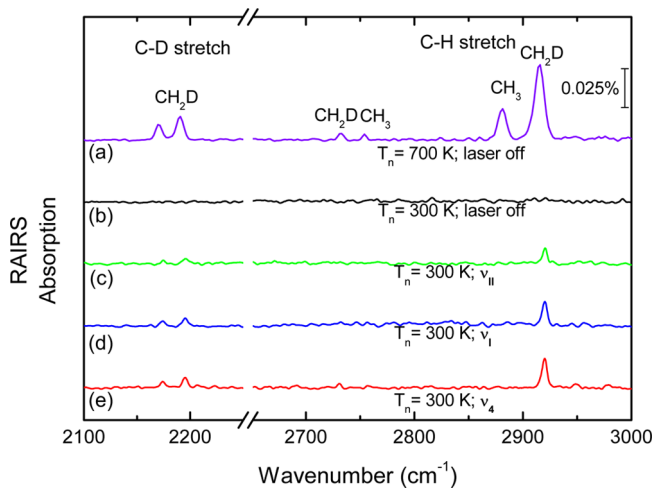


**Figure 1.** RAIR spectra of CH<sub>3</sub>D dissociation products on a Pt(111) surface at a surface temperature of 150 K. The peak assignments are given in spectrum a recorded for deposition from a hot nozzle (700 K,  $E_t = 49$  kJ/mol) resulting in both C–H and C–D bond cleavage. With the nozzle 300 K and  $E_t = 24 \pm 4.5$  kJ/mol, dissociation is only observed for the laser excited molecular beam. The three vibrational quantum states probed all lead to bond-selective C–H cleavage.

bond-selective and mode-specific character of the dissociation for C–H stretch excited CH<sub>3</sub>D. In the laser-off spectrum (a) taken with a nozzle temperature of 700 K, we observe RAIRS peaks due to both CH<sub>3</sub>(ads) and CH<sub>2</sub>D(ads), produced via C–D and C–H bond cleavage, respectively. The laser-off branching ratio determined from calibrated RAIRS signals is 22% C–D cleavage and 78% C–H cleavage, close to the

statistical limit of 1:3.<sup>4</sup> Figure 1b shows a laser-off RAIR spectrum for  $T_n = 300$  K, indicating that no dissociation occurs at this lower nozzle temperature without vibrational excitation via IR excitation. Figure 1c,d,e shows three RAIRS spectra for incident  $\text{CH}_3\text{D}$  prepared in three different vibrational states, labeled as  $\nu_I$ ,  $\nu_{II}$ , and  $\nu_4$ . In all three laser-on experiments, we observed exclusively the  $\text{CH}_2\text{D}(\text{ads})$  dissociation products and no evidence for C–D cleavage, indicating strong bond selectivity for C–H cleavage. Hence, excitation of  $\text{CH}_3\text{D}$  with one quantum of either the antisymmetric stretch ( $\nu_4$ ) or the symmetric stretch/bend overtone mixed eigenstates ( $\nu_I$  and  $\nu_{II}$ ) activates only the C–H cleavage reaction channel. The fact that the  $\text{CH}_2\text{D}$  absorption peak heights are different in Figure 1c,d,e for identical depositions (incident dose 95 ML of state prepared  $\text{CH}_3\text{D}$ ) indicates mode-specific reactivity for the three states probed here. The  $\text{CH}_2\text{D}$  peaks in (c)–(e) are smaller than those in (a) because spectrum (a) was taken after saturation of the surface.

Figure 2 shows the state-resolved uptake curves of the C–H cleavage product  $\text{CH}_2\text{D}(\text{ads})$  measured by RAIRS during a

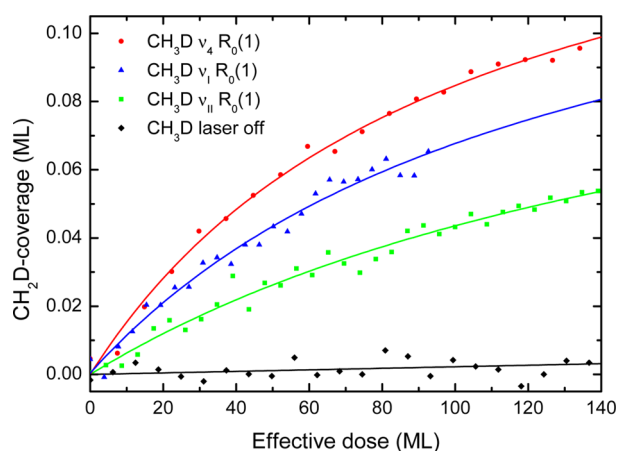


**Figure 2.** State-resolved uptake curves  $\theta(D)$  for  $\text{CH}_2\text{D}(\text{ads})$  on Pt(111) at  $T_s = 150$  K. The state-resolved initial sticking coefficient  $S_0$  is determined from the initial slopes of the uptake curves  $\theta(D)$  fitted to the data (see text). The effective dose measures the incident flux for each quantum state prepared by IR pumping, as determined by a pyroelectric detector inserted into the molecular beam.

deposition experiment on Pt(111). The state-resolved reactivity is proportional to the slope of the uptake curve. We fit an analytical uptake model to the data based on the Langmuir form

$$\theta(D) = A \cdot \frac{B \cdot D}{1 + B \cdot D}$$

where  $D$  is the incident dose,  $A$  is the saturation coverage, and  $B$  is a fitting constant. The coverage dependent sticking coefficient  $S(\theta)$  is given by  $\partial\theta/\partial D$ , the derivative of the fitted uptake curve  $\theta(D)$  with respect to the dose  $D$ . The initial slope (for  $D = 0$ ) corresponds to the initial sticking coefficient  $S_0$  on the clean Pt(111) surface and is given by  $A \cdot B$ . The analysis of the state-resolved uptake data shown in Figure 2 yields different initial sticking coefficients for the three different quantum states of  $\text{CH}_3\text{D}$  prepared by IR pumping as indicated by their different initial slope (see Table 1).

It should be noted that we also observe a variation in the saturation coverage for the three vibrational states, where the

**Table 1.** Sticking Coefficients and Saturation Coverages for Three Different Ro-vibrationally Excited Eigenstates of  $\text{CH}_3\text{D}$  ( $E_t = 24 \pm 4.5$  kJ/mol,  $T_s = 150$  K)

eigenstate	$S_0$	saturation coverage $\theta$
$\nu_I$	$(1.3 \pm 0.4) \times 10^{-3}$	$0.13 \pm 0.01$
$\nu_{II}$	$(0.7 \pm 0.3) \times 10^{-3}$	$0.13 \pm 0.02$
$\nu_4$	$(1.7 \pm 0.5) \times 10^{-3}$	$0.17 \pm 0.01$

state with the largest reactivity results in the largest saturation coverage. A recent combined experiment/theory study reported such an increase in  $\text{CH}_2\text{D}$  saturation coverage with increasing reactivity and found it to be due to a coverage dependent reaction barrier.<sup>24</sup>

Due to a strong Fermi resonance between the normal modes  $\nu_I$  (symmetric C–H stretch) and  $2\nu_5$  (C–H bending overtone) of  $\text{CH}_3\text{D}$ , the vibrational eigenstates  $|\nu_I\rangle$  and  $|\nu_{II}\rangle$  prepared by IR pumping with a single mode laser correspond to a mixture of the  $\nu_I$  and  $2\nu_5$  modes with different relative contributions. Wang et al. have developed an ab initio potential energy surface for  $\text{CH}_3\text{D}$  and calculated its vibrational states up to  $9000$   $\text{cm}^{-1}$ . Their calculations<sup>25,26</sup> identify the  $\text{CH}_3\text{D}$  eigenstates  $|\nu_I\rangle$  at  $2969.5$   $\text{cm}^{-1}$  and  $|\nu_{II}\rangle$  at  $2910$   $\text{cm}^{-1}$  in terms of a normal mode expansion with the leading terms given by  $|\nu_I\rangle = 0.77 \nu_I + 0.63 2\nu_5$  and  $|\nu_{II}\rangle = 0.63 \nu_I + 0.77 2\nu_5$ , indicating that these contain 60% stretch and 40% bending motion and vice versa. The third state at  $3016$   $\text{cm}^{-1}$ , in contrast, is a nearly pure antisymmetric C–H stretch normal mode  $\nu_4$  (96%). To further analyze the mode-specific behavior of the reactions, we calculate the hypothetical reactivities of the zero-order vibrational states  $\nu_I$  and  $2\nu_5$ . Simply inserting the measured  $|\nu_I\rangle$  and  $|\nu_{II}\rangle$  reactivities and solving the system of equations resulted in a small but negative reactivity for the pure  $2\nu_5$  state. We decided to rather follow the analysis of Yoon et al., who measured the relative reactivity  $\text{CH}_3\text{D}$  prepared in the same three eigenstates  $|\nu_I\rangle$ ,  $|\nu_{II}\rangle$  and  $\nu_4$  for the bimolecular collision with a chlorine atom.<sup>8</sup> Yoon et al. made the implicit assumption that the reactivities of the mixed eigenstates can be described as linear combinations of the reactivities of the zero-order states if they are scaled by the respective mixing factors (60% and 40%).

Because a hydrogen atom abstraction reaction is considered (in both this work and ref 8), it is plausible to assume that bending vibration  $2\nu_5$  does not promote reactivity. Thus, the reactivities will be proportional to the content of reactive zero-order stretching state in the excited eigenstate. Hence we can write the ratio of measured reactivities as

$$\frac{S_0^{|\nu_I\rangle}}{S_0^{|\nu_4\rangle}} = \frac{(1.3 \pm 0.4) \times 10^{-3}}{(1.7 \pm 0.5) \times 10^{-3}} = \frac{0.5929 \cdot S_0^{\nu_I}}{0.96 \cdot S_0^{\nu_4}}$$

Therefore, we can find the ratio of the sticking coefficients for the zero-order symmetric stretch excitation to antisymmetric stretch to be

$$\frac{S_0^{\nu_I}}{S_0^{\nu_4}} = 1.23 \pm 0.4$$

The consistency of this analysis can be tested by using the measured sticking coefficient for the  $|\nu_I\rangle$  eigenstate to predict that of the  $|\nu_{II}\rangle$  eigenstate.

$$\frac{S_0^{|\nu_I\rangle}}{S_0^{|\nu_{II}\rangle}} = \frac{0.5929}{0.3969} = 1.5$$



So the predicted  $\langle \nu_{\text{II}} \rangle$  reactivity of  $S_0^{\langle \nu_{\text{II}} \rangle - \text{calc}} = (0.9 \pm 0.3) \times 10^{-3}$ , which is in good agreement with the experimental result of  $S_0^{\langle \nu_{\text{II}} \rangle} = (0.7 \pm 0.3) \times 10^{-3}$ . The fact that the predicted reactivity is larger than the measured one, indicates that this analysis does not underestimate the  $2\nu_5$  reactivity. Therefore, the analysis is consistent and the initial assumption of a nonreactive bending overtone is justified. The deduced zero-order reactivities are summarized with the  $\text{CH}_2\text{D}_2$  reactivities in Table 2.

**Table 2. Eigenstate-Resolved Reactivities on Pt(111) at  $T_s = 150$  K and Translational Energies of  $24 \pm 4.5$  kJ/mol**

molecule	zero-order state	$S_0$
$\text{CH}_3\text{D}$	$\nu_1$	$(2.2 \pm 0.5) \times 10^{-3}$
$\text{CH}_3\text{D}$	$\nu_4$	$(1.8 \pm 0.2) \times 10^{-3}$
$\text{CH}_2\text{D}_2$	$\nu_1$	$(2.02 \pm 0.09) \times 10^{-3}$
$\text{CH}_2\text{D}_2$	$\nu_6$	$(1.47 \pm 0.07) \times 10^{-3}$

Despite the fact that this analysis yields consistent results, one has to be aware of the considerable simplifications that are introduced by assuming zero reactivity for the  $2\nu_5$  mode. It has been shown previously for  $\text{CH}_4$  dissociation on Pt(110)-(1 $\times$ 2) that the efficacies of different vibrations cannot be simply added to calculate the efficacies of combination bands.<sup>16</sup> Therefore, the reactivities of the zero-order states in  $\langle \nu_{\text{I}} \rangle$  and  $\langle \nu_{\text{II}} \rangle$  might influence each other differently for the different mixing ratios. In addition, calculations suggest that bending vibrations can increase reactivity, for example, for  $\text{CH}_4$  on Ni(111).<sup>27</sup> Nevertheless, the consistency of the analysis shows that the initial approximations are justifiable.

**State-Resolved Dissociation of  $\text{CH}_2\text{D}_2$  on Pt(111).** The dissociation of C–H stretch excited  $\text{CH}_2\text{D}_2$  was also found to be bond-selective both for excitation of the antisymmetric ( $\nu_6$ ) and for the symmetric C–H stretch ( $\nu_1$ ). The RAIRS spectra of the products of  $\text{CH}_2\text{D}_2$  dissociation on Pt(111) are shown in Figure 3. Spectrum (a) at the top was obtained for deposition from a hot nozzle ( $T_n = 700$  K) with a translational energy of

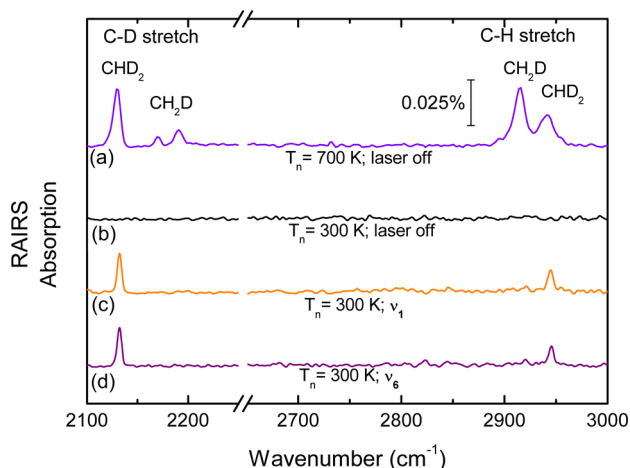


**Figure 3.** RAIR spectra of  $\text{CH}_2\text{D}_2$  dissociation products on a Pt(111) surface at a surface temperature of 150 K. The peak assignments are given in spectrum a recorded for deposition from a hot nozzle (700 K,  $E_t = 49$  kJ/mol) resulting in both CH and CD bond cleavage. With the nozzle 300 K and  $E_t = 24 \pm 4.5$  kJ/mol, dissociation is only observed for the laser excited molecular beam. The two quantum states probed all lead to bond-selective CH cleavage.

49 kJ/mol.<sup>4</sup> Both C–H and C–D cleavage products are observed in this case with a branching ratio of 55% CH cleavage and 45% CD cleavage, close to the statistical limit of 1:1. The laser-off spectrum recorded at a nozzle temperature of 300 K did not show any reactivity on the time scale of the experiment ( $\approx 1$  h). With IR pumping of either the symmetric C–H stretch ( $\nu_1$ ) or the antisymmetric C–H stretch mode  $\nu_6$  we detect only the C–H cleavage product  $\text{CHD}_2(\text{ads})$ , indicating strong bond selectivity upon C–H stretch excitation.

Figure 4 shows uptake curves of  $\text{CHD}_2$  that were obtained by monitoring the RAIRS absorption peak height of the C–H

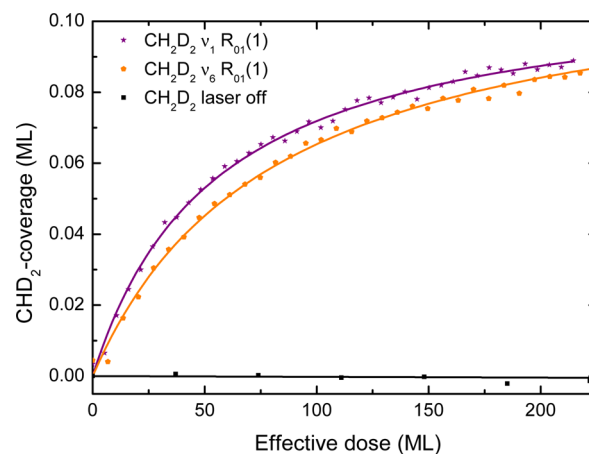


**Figure 4.** Uptake curves of  $\text{CHD}_2$  on Pt(111) as  $\text{CH}_2\text{D}_2$  dissociation product. The steeper initial slope of the  $\nu_1$  curve indicates a higher initial sticking coefficient  $S_0$  by a factor 1.4.

stretch peak of  $\text{CHD}_2$ . The steeper initial slope of the uptake curve for the  $\nu_1$ -excited  $\text{CH}_2\text{D}_2$  indicates that the  $\nu_1$ -excited molecules are 1.4 times more reactive than the  $\nu_6$ -excited molecules.

## DISCUSSION

Our observation that both  $\text{CH}_3\text{D}$  and  $\text{CH}_2\text{D}_2$  dissociate bond selectively if excited to vibrational eigenstates comprising C–H stretch and bend amplitude indicates that any intramolecular vibrational redistribution (IVR) that might occur between the laser preparation and the dissociation of the molecule is absent or at least incomplete. No IVR can occur during the typically 100  $\mu\text{s}$  flight time between laser preparation region and the approach to the surface in our apparatus because excitation by the cw-IR OPO (line width  $< 1$  MHz) prepares a single rovibrational eigenstate of the reactant molecule that has no time dependence and cannot undergo IVR. Once the reactant molecule enters the range of any molecule/surface interactions ( $d < 1$  nm), surface-induced IVR<sup>28</sup> may start to occur during the remaining time needed for the molecule to reach the transition state. At the incident speed used in the experiments described here, this flight time within range of molecule/surface interactions is less than 500 fs. Apparently, the time window available for surface-induced IVR is too short or the interactions too weak to allow for vibrational energy transfer between the C–H and C–D oscillators leading to bond-selective dissociation upon C–H stretch and bend excitation.

The experimentally observed bond selectivity is in disagreement with the prediction of statistical models for the dissociation of methane on Pt(111).<sup>29,30</sup> These models assume randomization of the initial vibrational energy due to rapid

intramolecular energy transfer within a short-lived complex formed with surface atoms before the C–H bond breaks and therefore exclude mode-specific and bond-selective dissociation of methane.

Both CH<sub>2</sub>D<sub>2</sub> and CH<sub>3</sub>D show mode-specific dissociation where the symmetric stretching vibration is more reactive than the antisymmetric C–H stretching. Yoon et al.<sup>8</sup> who studied the reaction of CH<sub>3</sub>D with chlorine atoms in the gas phase performed ab initio calculations to rationalize the difference in reactivity observed for reactant preparation in the  $\nu_4$  and  $\nu_1$  modes. They calculated the evolution of the vibrational frequencies as the CH<sub>3</sub>D molecule approached the Cl atom and found that the vibrational frequency of the  $\nu_1$  mode was reduced significantly, leading to a reduction in dissociation barrier height whereas the frequency of the  $\nu_4$  mode stayed nearly constant throughout the approach of the reactants. Furthermore, for the  $\nu_1$  vibration, the vibrational amplitude of three C–H stretch oscillators became localized in the reactive C–H bond pointing toward the Cl atom. In contrast, the vibrational amplitude of the  $\nu_4$  vibration remained quarantined in the two C–H oscillators pointing away from the reaction partner.

Similarly, for molecule–surface reactions, the interaction of the incident molecule with a metal surface can lead to surface-induced intramolecular vibration redistribution (IVR), which could lead to vibrational mode specificity due to differences in the localization of vibrational energy for different initial vibrational states. Halonen et al.<sup>31</sup> proposed a simple model for this process, which calculates the evolution of the C–H stretch modes as a nonrotating CH<sub>4</sub> approaches a metal surface with a single C–H bond pointing toward the surface. The model predicts that the symmetric stretch ( $\nu_1$ ) of CH<sub>4</sub> transforms adiabatically into excitation of the single C–H oscillator pointing toward the metal surface. The antisymmetric CH<sub>4</sub> stretch mode  $\nu_3$ , however, is predicted to evolve adiabatically to the excitation of the methyl group, pointing away from the surface. On the basis of the different localization of the vibrational energy for the two initial states, Halonen et al. predicted a larger effect of  $\nu_1$  excitation on the CH<sub>4</sub> reactivity compared to the effect of the initial  $\nu_3$  excitation. State-resolved reactivity measurements<sup>15,32</sup> for CH<sub>4</sub>( $\nu_1$ ) and CH<sub>4</sub>( $\nu_3$ ) later confirmed the prediction of this simple model.

More recently, Bret Jackson developed a dynamical model for CH<sub>4</sub> chemisorption on transition metals,<sup>33,34</sup> which includes all internal modes of methane as well as rotation and surface atom motion. Jackson's reaction path Hamiltonian model<sup>33,34</sup> predicts higher reactivity for initial excitation of the symmetric C–H stretch mode  $\nu_1$  due to stronger mode softening and lowering the vibrational adiabatic dissociation barrier for  $\nu_1$  than for the other normal modes. In addition, vibrationally nonadiabatic transitions to the vibrational state of lower energy can convert vibrational energy into translational motion along the reaction coordinate, leading to mode-specific enhancement of the reactivity. Such mode-specific surface-induced IVR is also possible for the reaction of CH<sub>3</sub>D and CH<sub>2</sub>D<sub>2</sub> with a Pt(111) surface if the initially prepared states evolve differently during the reactant's approach to the surface, leading to different degrees of vibrational amplitude localization and different reactivities.

Alternatively, the so-called sudden vector projection model (SVP) was recently proposed by some of the current authors<sup>20,21</sup> to explain and predict vibrational mode specificity and bond selectivity both in bimolecular gas-phase and in gas–

surface reactions. The SVP model assumes that IVR within the reactants is much slower than the time scale of the reactive collision and therefore treats the reaction as sudden; i.e., it neglects the surface-induced IVR processes that are calculated in Jackson's RPH model. The SVP model simply calculates the overlap of the reactant's normal mode vectors with the corresponding reaction coordinate at the appropriate transition state.<sup>18,19</sup> The application of this model to various gas-phase<sup>20</sup> and gas–surface reactions<sup>35</sup> has generally been successful. In particular, it predicted successfully the observed strong bond selectivity in the chemisorption of deuterated methanes on Ni(111).<sup>19</sup>

In Table 3, the SVP values have been computed for the dissociation of CH<sub>3</sub>D and CH<sub>2</sub>D<sub>2</sub> on Pt(111), using the

**Table 3. Sudden Vector Projections of the Reactant Vibrational and Translational Modes onto the Reaction Coordinate at the Transition State<sup>a</sup>**

mode	CH <sub>3</sub> D	CH <sub>2</sub> D <sub>2</sub>
	H + CH <sub>2</sub> D/D + CH <sub>3</sub>	H + CHD <sub>2</sub> /D + CH <sub>2</sub> D
$\nu_1$	0.44/0.04	0.57/0.04
$\nu_2$	0.04/0.71	0.06/0.48
$\nu_3$	0.29/0.05	0.30/0.09
$\nu_4$	0.38/0.01	0.03/0.32
$\nu_5$	0.24/0.15	0.36/0.31
$\nu_6$	0.14/0.24	0.48/0.02
$\nu_7$		0.12/0.31
$\nu_8$		0.02/0.53
$\nu_9$		0.31/0.07
trans X	0.006/0.02	0.005/0.01
trans Y	0.003/0.01	0.005/0.005
trans Z	0.32/0.39	0.32/0.40

<sup>a</sup>C–H and C–D cleavage channels are identified by the corresponding C–H or C–D bond elongated at the transition state.

protocol described in ref 36, directly from density functional theory calculations implemented in Vienna ab initio simulation package (VASP).<sup>37,38</sup> Briefly, the Pt(111) surface was modeled with a five-layer slab and the methane molecule was placed above a 3 × 3 (1/9 ML coverage) surface unit cell. The interaction between the ionic cores and electrons was described with the projector-augmented wave (PAW) method,<sup>39</sup> and the Kohn–Sham valence electronic wave function was expanded in a plane-wave basis set<sup>40</sup> with a cutoff at 350 eV. The Brillouin zone was sampled with a 4 × 4 × 1  $\gamma$ -centered  $k$ -points grid. The generalized gradient approximation (GGA) was used to treat the electron exchange–correlation effects with the Perdew–Burke–Ernzerhof (PBE)<sup>41</sup> functional. The top three layers were relaxed during optimization and the transition state was found by the climbing-image nudged elastic band method,<sup>42</sup> followed by the normal-mode analysis to confirm a single imaginary frequency. The reactant geometry was obtained by separating the molecule and the surface in the direction of the surface normal, and then optimizing the transition state geometry to the equilibrium geometry of methane with little reorientation. The SVP values were then determined as the overlaps between reactant vibrational normal mode vectors and the vector of reaction coordinate at transition state corresponding to the imaginary frequency.

It is clear from the table that the SVP model is in general agreement with the mode specificity and bond selectivity observed in the experiment. For CH<sub>3</sub>D dissociation, for

example, the observation that the excitation of CH<sub>3</sub>D in C–H stretch modes ( $\nu_1$  and  $\nu_4$ ) only promotes the CH cleavage reaction channel is in agreement with the much larger SVP values for this channel over the CD cleavage channel. In addition, the SVP for  $\nu_1$  is slightly larger than for  $\nu_4$ , again corresponding well to the slightly higher reactivity of symmetric C–H stretch mode  $\nu_1$  compared to that of the antisymmetric C–H stretch mode  $\nu_4$ . It is also predicted that the excitation of C–D stretch modes would substantially activate the CD cleavage channel without promotion of the CH cleavage channel, similar to the highly bond-selective behavior due to the C–H stretch excitation in CHD<sub>3</sub> dissociative chemisorption.<sup>3,4,43</sup> Furthermore, for the CH<sub>2</sub>D<sub>2</sub> molecule, the SVP model successfully reproduces the strongly bond-selective CH cleavage due to the excitation of C–H stretch modes  $\nu_1$  and  $\nu_6$ , and the slight reactivity preference of  $\nu_1$  over  $\nu_6$ . It is also suggested that the excitation of C–D stretch modes  $\nu_2$  and  $\nu_8$  would selectively enhance the C–D cleavage channel. However, the prediction of the SVP model to the bending modes could be less reliable, and the influence of bending overtones (e.g., the  $2\nu_5$  state in CH<sub>3</sub>D and the  $2\nu_3$  state in CH<sub>2</sub>D<sub>2</sub>) may be better investigated by dynamical calculations on a global potential energy surface.

## CONCLUSIONS

We measured the reaction probabilities for the dissociative chemisorption of CH<sub>3</sub>D and CH<sub>2</sub>D<sub>2</sub> on a clean Pt(111) surface for several vibrational eigenstates. For vibrational excitation comprising C–H stretch excitation, the reactions are observed to be both mode-specific and bond-selective. Calculation of the normal mode reaction probabilities from the measured reactivities of the mixed eigenstates of CH<sub>3</sub>D  $|v_1\rangle$  and  $|v_{11}\rangle$  shows that the pure symmetric stretching vibration promotes reactivity more than the pure antisymmetric stretch. Analogous results were observed in the case of CH<sub>2</sub>D<sub>2</sub>. These results show that surface-induced IVR between C–H and C–D stretch modes is absent or incomplete on the time scale of the molecule/surface collision, leading to bond-specific dissociation.

To understand the origin of the observed mode specificity and bond selectivity, we have relied on the recently proposed SVP model. Assuming the collision time to be much shorter than the time needed for IVR, the SVP model attributes the ability of a reactant mode for enhancing the reactivity into a particular product channel to its overlap with the reaction coordinate of the corresponding transition state. The SVP model correctly predicted the experimental trends, revealing the different coupling strengths of the various vibrational modes of these two deuterated methane molecules with the reaction coordinate of the respective transition states.

## AUTHOR INFORMATION

### Present Addresses

<sup>§</sup>Swiss Federal Laboratories for Materials Science and Technology.

<sup>||</sup>National Institute for Materials Science (NIMS), Ibaraki, 305-0047, Japan.

### Notes

The authors declare no competing financial interest.

## ACKNOWLEDGMENTS

R.D.B. gratefully acknowledges financial support provided by the Swiss National Science Foundation (Grant No. 159689/1) and the Ecole Polytechnique Fédérale de Lausanne. H.G. thanks the U.S. National Science Foundation (Grant No. CHE-1462109) for generous support.

## REFERENCES

- (1) Crim, F. F. Vibrational state control of bimolecular reactions: Discovering and directing the chemistry. *Acc. Chem. Res.* **1999**, *32* (10), 877–884.
- (2) Zare, R. N. Laser control of chemical reactions. *Science* **1998**, *279* (5358), 1875–1879.
- (3) Killelea, D. R.; Campbell, V. L.; Shuman, N. S.; Utz, A. L. Bond-selective control of a heterogeneously catalyzed reaction. *Science* **2008**, *319* (5864), 790–793.
- (4) Chen, L.; Ueta, H.; Bisson, R.; Beck, R. D. Vibrationally bond-selected chemisorption of methane isotopologues on Pt(111) studied by reflection absorption infrared spectroscopy. *Faraday Discuss.* **2012**, *157*, 285–295.
- (5) Nattino, F.; Ueta, H.; Chadwick, H.; van Reijzen, M. E.; Beck, R. D.; Jackson, B.; van Hemert, M. C.; Kroes, G.-J. Ab initio molecular dynamics calculations versus quantum-state-resolved experiments on CHD<sub>3</sub> + Pt(111): new insights into a prototypical gas–surface reaction. *J. Phys. Chem. Lett.* **2014**, *5*, 1294–1299.
- (6) Chorkendorff, I.; Niemantsverdriet, J. W. *Concepts of modern catalysis and kinetics*; Wiley-VCH: New York, 2003.
- (7) Sinha, A.; Hsiao, M. C.; Crim, F. F. Bond-selected bimolecular chemistry - H+HOD( $\nu_{OH}$ )-OD+H<sub>2</sub>. *J. Chem. Phys.* **1990**, *92* (10), 6333–6335.
- (8) Yoon, S.; Holiday, R. J.; Sibert, E. L.; Crim, F. F. The relative reactivity of CH<sub>3</sub>D molecules with excited symmetric and antisymmetric stretching vibrations. *J. Chem. Phys.* **2003**, *119* (18), 9568–9575.
- (9) Yoon, S.; Henton, S.; Zivkovic, A. N.; Crim, F. F. The relative reactivity of the stretch-bend combination vibrations of CH<sub>4</sub> in the Cl(<sup>2</sup>P<sub>3/2</sub>)+CH<sub>4</sub> reaction. *J. Chem. Phys.* **2002**, *116* (24), 10744–10752.
- (10) Yoon, S.; Holiday, R. J.; Crim, F. F. Control of bimolecular reactions: Bond-selected reaction of vibrationally excited CH<sub>3</sub>D with Cl(<sup>2</sup>P<sub>3/2</sub>). *J. Chem. Phys.* **2003**, *119* (9), 4755–4761.
- (11) Kim, Z. H.; Bechtel, H. A.; Zare, R. N. Vibrational control in the reaction of methane with atomic chlorine. *J. Am. Chem. Soc.* **2001**, *123* (50), 12714–12715.
- (12) Bechtel, H. A.; Kim, Z. H.; Camden, J. P.; Zare, R. N. Bond and mode selectivity in the reaction of atomic chlorine with vibrationally excited CH<sub>2</sub>D<sub>2</sub>. *J. Chem. Phys.* **2004**, *120* (2), 791–799.
- (13) Beck, R. D.; Maroni, P.; Papageorgopoulos, D. C.; Dang, T. T.; Schmid, M. P.; Rizzo, T. R. Vibrational mode-specific reaction of methane on a nickel surface. *Science* **2003**, *302* (5642), 98–100.
- (14) Juurlink, L. B. F.; Smith, R. R.; Killelea, D. R.; Utz, A. L. Comparative study of C-H stretch and bend vibrations in methane activation on Ni(100) and Ni(111). *Phys. Rev. Lett.* **2005**, *94* (20), 208303.
- (15) Maroni, P.; Papageorgopoulos, D. C.; Sacchi, M.; Dang, T. T.; Beck, R. D.; Rizzo, T. R. State-resolved gas-surface reactivity of methane in the symmetric C-H stretch vibration on Ni(100). *Phys. Rev. Lett.* **2005**, *94* (24), 246104.
- (16) Bisson, R.; Sacchi, M.; Beck, R. D. Mode-specific reactivity of CH<sub>4</sub> on Pt(110)-(1 × 2): The concerted role of stretch and bend excitation. *Phys. Rev. B: Condens. Matter Mater. Phys.* **2010**, *82* (12), 121404.
- (17) Hundt, P. M.; van Reijzen, M. E.; Ueta, H.; Beck, R. D. Vibrational activation of methane chemisorption: the role of symmetry. *J. Phys. Chem. Lett.* **2014**, *5* (11), 1963–1967.
- (18) Jiang, B.; Liu, R.; Li, J.; Xie, D. Q.; Yang, M. H.; Guo, H. Mode selectivity in methane dissociative chemisorption on Ni(111). *Chem. Sci.* **2013**, *4* (8), 3249–3254.



- (19) Jiang, B.; Guo, H. Mode and bond selectivities in methane dissociative chemisorption: quasi-classical trajectory studies on twelve-dimensional potential energy surface. *J. Phys. Chem. C* **2013**, *117* (31), 16127–16135.
- (20) Guo, H.; Jiang, B. The sudden vector projection model for reactivity: mode specificity and bond selectivity made simple. *Acc. Chem. Res.* **2014**, *47* (12), 3679–3685.
- (21) Jiang, B.; Guo, H. Relative efficacy of vibrational vs. translational excitation in promoting atom-diatom reactivity: Rigorous examination of Polanyi's rules and proposition of sudden vector projection (SVP) model. *J. Chem. Phys.* **2013**, *138* (23), 234104.
- (22) Chen, L.; Ueta, H.; Bisson, R.; Beck, R. D. Quantum state-resolved gas/surface reaction dynamics probed by reflection absorption infrared spectroscopy. *Rev. Sci. Instrum.* **2013**, *84* (5), 053902.
- (23) Chadwick, H.; Hundt, P. M.; van Reijzen, M. E.; Yoder, B. L.; Beck, R. D. Quantum state specific reactant preparation in a molecular beam by rapid adiabatic passage. *J. Chem. Phys.* **2014**, *140* (3), 034321.
- (24) Ueta, H.; Chen, L.; Beck, R. D.; Colon-Diaz, I.; Jackson, B. Quantum state-resolved CH<sub>4</sub> dissociation on Pt(111): coverage dependent barrier heights from experiment and density functional theory. *Phys. Chem. Chem. Phys.* **2013**, *15* (47), 20526–20535.
- (25) Wilmshurst, J. K.; Bernstein, H. J. The infrared spectra of CH<sub>4</sub>, CH<sub>3</sub>D, CH<sub>2</sub>D<sub>2</sub>, CD<sub>3</sub>H, and CD<sub>4</sub>. *Can. J. Chem.* **1957**, *35* (3), 226–235.
- (26) Wang, X. G.; Sibert, E. L. A nine-dimensional perturbative treatment of the vibrations of methane and its isotopomers. *J. Chem. Phys.* **1999**, *111* (10), 4510–4522.
- (27) Jackson, B.; Nave, S. The dissociative chemisorption of methane on Ni(111): The effects of molecular vibration and lattice motion. *J. Chem. Phys.* **2013**, *138* (17), 174705.
- (28) Killelea, D. R.; Utz, A. L. On the origin of mode- and bond-selectivity in vibrationally mediated reactions on surfaces. *Phys. Chem. Chem. Phys.* **2013**, *15* (47), 20545–20554.
- (29) Ukraintsev, V. A.; Harrison, I. A statistical-model for activated dissociative adsorption - application to methane dissociation on Pt(111). *J. Chem. Phys.* **1994**, *101* (2), 1564–1581.
- (30) Bukoski, A.; Blumling, D.; Harrison, I. Microcanonical unimolecular rate theory at surfaces. I. Dissociative chemisorption of methane on Pt(111). *J. Chem. Phys.* **2003**, *118* (2), 843–871.
- (31) Halonen, L.; Bernasek, S. L.; Nesbitt, D. J. Reactivity of vibrationally excited methane on nickel surfaces. *J. Chem. Phys.* **2001**, *115* (12), 5611–5619.
- (32) Smith, R. R.; Killelea, D. R.; DelSesto, D. F.; Utz, A. L. Preference for vibrational over translational energy in a gas-surface reaction. *Science* **2004**, *304* (5673), 992–995.
- (33) Jackson, B.; Nave, S. The dissociative chemisorption of methane on Ni(100): Reaction path description of mode-selective chemistry. *J. Chem. Phys.* **2011**, *135* (11), 114701.
- (34) Guo, H.; Jackson, B. Mode- and bond-selective chemistry on metal surfaces: the dissociative chemisorption of CHD<sub>3</sub> on Ni(111). *J. Phys. Chem. C* **2015**, *119* (26), 14769–14779.
- (35) Jiang, B.; Yang, M.; Xie, D.; Guo, H. Quantum dynamics of polyatomic dissociative chemisorption on transition metal surfaces: mode specificity and bond selectivity. *Chem. Soc. Rev.* **2015**, DOI: 10.1039/C5CS00360A.
- (36) Jiang, B.; Guo, H. Prediction of mode specificity, bond selectivity, normal scaling, and surface lattice effects in water dissociative chemisorption on several metal surfaces using the sudden vector projection model. *J. Phys. Chem. C* **2014**, *118* (46), 26851–26858.
- (37) Kresse, G.; Furthmüller, J. Efficient iterative schemes for ab initio total-energy calculations using plane wave basis set. *Phys. Rev. B: Condens. Matter Mater. Phys.* **1996**, *54*, 11169–11186.
- (38) Kresse, G.; Furthmüller, J. Efficiency of ab initio total energy calculations for metals and semiconductors using plane wave basis set. *Comput. Mater. Sci.* **1996**, *6*, 15–50.
- (39) Blochl, P. E. Project augmented-wave method. *Phys. Rev. B: Condens. Matter Mater. Phys.* **1994**, *50*, 17953–17979.
- (40) Kresse, G.; Joubert, D. From ultrasoft pseudopotentials to the projector augmented-wave method. *Phys. Rev. B: Condens. Matter Mater. Phys.* **1999**, *59*, 1758–1775.
- (41) Perdew, J. P.; Burke, K.; Ernzerhof, M. Generalized gradient approximation made simple. *Phys. Rev. Lett.* **1996**, *77* (18), 3865–3868.
- (42) Henkelman, G.; Uberuaga, B. P.; Jonsson, H. A climbing image nudged elastic band method for finding saddle points and minimum energy paths. *J. Chem. Phys.* **2000**, *113*, 9901–9904.
- (43) Shen, X. J.; Lozano, A.; Dong, W.; Busnengo, H. F.; Yan, X. H. Towards bond selective chemistry from first principles: methane on metal surfaces. *Phys. Rev. Lett.* **2014**, *112* (4), 046101.